Computational Analysis of Mo and W Oxoanions through Bond Order and Bonding Energy Approaches

Adam J. Bridgeman* and Germán Cavigliasso†

Department of Chemistry, University of Hull, Kingston upon Hull HU6 7RX, UK

Received: January 13, 2003; In Final Form: March 27, 2003

A detailed bonding analysis of Mo and W $[MO_4]^{2-}$, $[M_2O_7]^{2-}$, and $[M_6O_{19}]^{2-}$ anions has been carried out. The nature of the metal−oxygen interactions and the bonding properties of oxygen sites have been explored by combining population analysis, including bond and valency indexes, with information based on the composition of molecular orbitals and the calculation of bonding energetics. Particular attention has been focused on the effects of basis sets and functionals on the correlations between the various approaches. The results obtained from population analysis have been found to be qualitatively consistent with those provided by bonding-energy approaches for basis sets of triple-ζ quality and all functionals tested. Use of smaller basis sets has had only a relatively minor effect on the bonding-energy results but has led to some significant discrepancies in the population analysis.

1. Introduction

The success and popularity of density functional theory[1] as a method of calculating and describing the electronic structures of molecules and materials have been frequently attributed to computational features that provide a combination of practicality and accuracy that cannot be matched by conventional methods including electron correlation.

The conceptual aspects of density-functional theory have also been recognized as highly appealing from a chemical point of view, since several important universal concepts of molecular structure and reactivity, such as chemical potential, electronegativity, hardness and softness, reactivity indexes, are naturally involved in the density-functional language.[2]

The physical and chemical significance of the Kohn−Sham molecular orbitals has, nevertheless, been a rather controversial subject. The initial views of these orbitals as mathematical entities devoid of any useful analytical character have been disproved by rather extensive comparative investigations on the general properties of the Hartree−Fock (HF) and Kohn−Sham orbitals (KS) and their application to the calculation of atomic charge, bond index, and valence. The most important conclusions from these studies indicate that "the shape and symmetry properties of the KS orbitals are very similar to those calculated by the HF method",[3] and that "no appreciable difference is noticed between their performance in the theoretical study of bonding".[4]

In a recent article on the role of Kohn−Sham density functional theory as a tool for predicting and understanding chemistry, Bickelhaupt and Baerends[5] have considered that this method "not only offers a road to accurate calculation and prediction, but also allows interpretation and understanding of chemical bonding phenomena using elementary physical concepts". These authors have also described the combination of population analysis of molecular orbitals with the decomposition of the bonding energy into physically meaningful quantities as an excellent method for the study of the interactions between chemically useful fragments in a molecular structure.

In a detailed and extensive investigation of polyoxoanions formed by the transition elements Mo and W,[6−11] we have employed this combined approach based on population methods and bonding energetics, and in addition to the traditional analysis of molecular-orbital compositions and the calculation of (Mulliken) atomic charges, we have also incorporated computational bond orders and valency indexes. In particular, we have found that the combination of the bond and valency indexes with bonding-energy results can be a useful analytical and interpretative tool. The purpose of the present work is to further explore the general applicability of bond-order and bonding-energy methods by investigating how basis-set and functional dependence, and the choice of fragments, affect the correlations and complementary nature of these analytical techniques. The calculations concentrate on three groups of oxoanions of Mo and W: $[MO_4]^{2-}$, $[M_2O_7]^{2-}$, and $[M_6O_{19}]^{2-}$.

2. Computational Approach

A computational definition for the bond order (β_{AB}) between two atoms *A* and *B* has been proposed by Mayer[12] as an extension of Mulliken population analysis, as is given by

$$\beta_{AB} = \sum_{i\epsilon A}\sum_{j\epsilon B}(PS)_{ij}(PS)_{ji} \tag{1}$$

where the density matrix (P_{ij}) elements are defined by

$$P_{ij} = \sum_{k} C_{ik}{}^{*}C_{jk} \tag{2}$$

and the overlap matrix (S_{ij}) elements are

$$S_{ij} = \int g_i{}^{*}g_j \, d\mathbf{r} \tag{3}$$

The coefficients (C_{ik}) and atomic basis functions (g_i) are used

* Corresponding author. E-mail: A. J.Bridgeman@hull.ac.uk
† Present address: Department of Chemistry, Faculty of Science, Australian National University, Canberra ACT 0200 Australia. E-mail: German.Cavigliasso@anu.edu.au

10.1021/jp034078o CCC: $25.00
Published on Web 05/10/2003

in the construction of the molecular orbitals (φ_k) as a linear combination of atomic orbitals, that is,

$$\varphi_k = \sum_i g_i C_{ik} \tag{4}$$

Mayer bond orders and Mulliken atomic charges have been integrated in a definition of atomic valency, proposed by Evarestov and Veryazov,[13] which can be used as a combined measure of covalent (covalency) and ionic (electrovalency) bonding. The (full) valency (V) of atom A is defined as

$$V_A = \frac{1}{2}[C_A + (C_A{}^2 + 4Q_A{}^2)^{1/2}] \tag{5}$$

where C_A and Q_A are, respectively, the sum of the Mayer bond indexes and the Mulliken charge associated with atom A.

The covalency (C_A) index is defined as a sum of all Mayer bond orders for a given atom and therefore includes contributions (for example, from atoms not directly bonded to one another) that may be small but not necessarily negligible. This can be represented as

$$C_A = \sum \beta^b_{AB} + \sum \beta^n_{AB} \tag{6}$$

where the first term can be considered as a bond sum (S_{AB}) for atom A which involves the contributions from directly bonded atoms (B^b),

$$S_{AB} = \sum \beta^b_{AB} \tag{7}$$

and the second term represents the small contributions arising from secondary (largely nonbonding) interactions.

A computational analysis of bonding energetics can be carried out by decomposing the total bonding energy (E_B) of a molecular system as

$$E_B = E_O + E_P + E_E \tag{8}$$

where E_O, E_P, and E_E are, respectively, orbital-mixing, Pauli-repulsion, and electrostatic-interaction terms. Descriptions of the physical significance of these properties have been given by Landrum, Goldberg, and Hoffmann[14] and by Bickelhaupt and Baerends.[5]

The E_E component is calculated from the superposition of the atomic (ρ_i) densities at the molecular geometry,

$$\rho_E = \sum \rho_i \tag{9}$$

and represents the classical electrostatic effects associated with the interacting (fragment) charge distributions. The E_E contribution is primarily dominated by the nucleus-electron attractions, and therefore has a stabilizing influence. The E_P component is obtained by requiring that the (Pauli) antisymmetry conditions be satisfied. This leads to a destabilizing orbital contribution that has been described as a measure of steric repulsion. The E_O component represents a stabilizing factor originating from the relaxation of the molecular system due to the mixing of occupied and unoccupied orbitals, and involves the effects associated with electron-pair bonding, charge transfer or donor−acceptor interactions, and polarization.

Equation 8 corresponds to a molecular system described as a collection of neutral atomic fragments. If the molecular structure is generically decomposed as

$$[X] + [Y] + [Z] = [XYZ] \tag{10}$$

TABLE 1: Composition of Basis Sets, Given as Orbitals Included in the Core and Number of Valence Sets, of *s, p, d,* and *f* Type

element	core orbitals	valence functions	type
O	1s	2s 2p1d	DZ1P
		3s 3p 1d	TZ1P
		3s 3p 1d 1f	TZ2P
Mo	1s−3d	2s 2p 2d 2s 1p	DZ1P
		2s 3p 3d 3s 1p	TZ1P
		2s 3p 3d 3s 1p 1f	TZ2P
W	1s−4f	2s 2p 2d 2s 1p	DZ1P
		3s 3p 3d 3s 1p	TZ1P
		3s 3p 3d 3s 1p 1f	TZ2P

the total molecular bonding energy of the [XYZ] system relative to the separate [X], [Y], [Z] fragments is then given by

$$\Delta E_B = \Delta E_O + \Delta E_P + \Delta E_E \tag{11}$$

It should be noted that the fragments in eq 10 can take any chemical form, atom, ion, or molecule.

The magnitude of the orbital-mixing, Pauli, and electrostatic contributions to the bonding energy has been found to correlate with the extent of density and orbital overlap.[5] In general, the greater the interpenetration of the fragment charge distributions and the more strongly the fragment orbitals overlap with one another, the more favorable or less unfavorable the electrostatic and orbital-mixing effects are, respectively. In contrast, a more extensive orbital overlap leads to stronger Pauli repulsion due to the enhancement of destabilizing kinetic-energy effects.

3. Calculation Details

All density functional calculations reported in this work were performed with the ADF (2000.02)[15−19] program. Bond and valency indexes were obtained with a program[20] designed for their computation from the ADF output file. Graphics of molecular orbitals were generated with the MOLEKEL[21] program. Functionals based on the Vosko−Wilk−Nusair[22] (VWN) form of the local density approximation[23] (LDA) and on the gradient-corrected forms BP86, consisting of Becke (1988) exchange[24] and Perdew (1986) correlation[25] expressions, BLYP, consisting of Becke (1988) exchange and Lee−Yang−Parr correlation[26] expressions, and PW91, given by Perdew and Wang,[27] were utilized. Basis sets of double-ζ and triple-ζ quality incorporating frozen cores and the ZORA relativistic approach [19] were employed. The basis sets were combined in three different schemes labeled DZ1P, TZ1P, and TZ2P. Detailed descriptions are given in Table 1.

All results reported in this work correspond to optimized geometries obtained with an LDA/TZ1P[7,28,29] approach. The influence of basis sets and functionals on the computational properties investigated was probed by means of single-point calculations at these LDA/TZ1P geometries. Studies of basis-set effects were carried out using the LDA and BP86 functionals for population analysis and bonding energetics, respectively. Studies of functional effects on bonding-energy results were performed using the TZ1P basis sets. Previous investigations[30] have indicated that Mayer indexes appear to be largely insensitive to the functionals employed in the calculations, and therefore the functional dependence of the bond orders was not explored in this work.

4. Results and Discussion

4.1. Molecular Structures. Structural and atom-labeling schemes for the three groups of oxoanions studied in this work

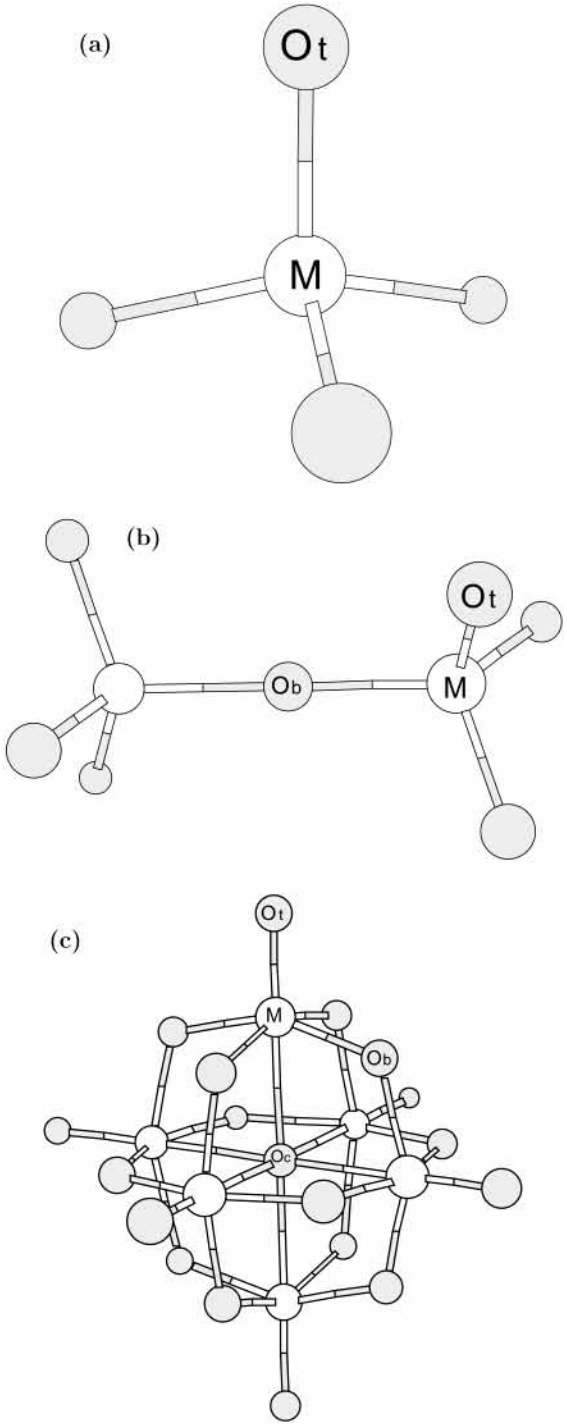

Figure 1. Structural and atom-labeling scheme for (a) $[MO_4]^{2-}$, (b) $[M_2O_7]^{2-}$, and (c) $[M_6O_{19}]^{2-}$ anions.

are given in Figure 1. The metal atoms in the $[MO_4]^{2-}$ and $[M_2O_7]^{2-}$ species lie in four-coordinate environments which possess regular tetrahedral (T_d) symmetry in the former, but are distorted in the latter due to the presence of longer bridging ($M-O_b$) than terminal ($M-O_t$) bonds.

The molecular structure of the $[M_2O_7]^{2-}$ anions can adopt a variety of configurations which correspond to the occurrence of linear or bent $[M-O_b-M]$ units and of eclipsed or staggered orientations of the $[MO_3]$ terminal groups. All of these configurations have been investigated in a previous work,[29] and it has been found that the possible conformers exhibit only minor differences in stability. However, the anions with linear bridges possess higher symmetry and are thus more convenient for analytical purposes. The structures with D_{3d} symmetry are considered in the present work.

TABLE 2: Optimized (LDA/TZ1P) Bond Distances (in pm) for $[MO_4]^{2-}$, $[M_2O_7]^{2-}$, and $[M_6O_{19}]^{2-}$ Anions

molecule	bond	result
$[MoO_4]^{2-}$	$M-O_t$	180
$[WO_4]^{2-}$	$M-O_t$	181
$[Mo_2O_7]^{2-}$	$M-O_t$	175
	$M-O_b$	190
$[W_2O_7]^{2-}$	$M-O_t$	177
	$M-O_b$	191
$[Mo_6O_{19}]^{2-}$	$M-O_t$	171
	$M-O_b$	193
	$M-O_c$	232
$[W_6O_{19}]^{2-}$	$M-O_t$	173
	$M-O_b$	194
	$M-O_c$	234

TABLE 3: Mulliken Analysis (LDA) of $[MO_4]^{2-}$ Anions[a]

		charge		population			
molecule	basis set	M	O	Ms	Mp	Md	Mf
$[MoO_4]^{2-}$	DZ1P	+1.79	−0.95	1.3	3.3	17.8	0.0
	TZ1P	+1.58	−0.90	1.3	3.0	17.9	0.0
	TZ2P	+1.38	−0.85	3.3	2.8	17.0	0.5
$[WO_4]^{2-}$	DZ1P	+1.97	−0.99	4.5	3.4	17.1	0.0
	TZ1P	+1.78	−0.94	4.2	2.9	17.4	0.0
	TZ2P	+1.59	−0.90	5.4	2.7	16.7	0.5

[a] The populations of metal basis functions are given as percentage per individual orbital.

The $[M_6O_{19}]^{2-}$ clusters differ from the smaller anions in that all metal atoms are six-coordinate. The molecular structure possesses ideal octahedral (O_h) symmetry, but the local environment of the Mo and W sites is a distorted polyhedron of C_{4v} symmetry. The metal atoms are all equivalent, whereas three different groups of oxygen sites are observed. These are represented by terminal (O_t), bridging (O_b), and central (O_c) atoms.

Bond distances calculated using an LDA/TZ1P approach are reproduced in Table 2. These data have been taken from previous work on the $[MO_4]^{2-}$,[28] $[M_2O_7]^{2-}$,[29] and $[M_6O_{19}]^{2-}$ [7] anions, and comparisons with available experimental results can be found in the original publications. In all cases, the computational−experimental agreement has been found to be satisfactory.

4.2. $[MO_4]^{2-}$ Anions. A qualitative molecular-orbital diagram showing the metal−oxygen interactions that are most important to chemical bonding in the $[MO_4]^{2-}$ anions is given in Figure 2. The highest-occupied ($1t_1$) level (HOMO) represents the only group of orbitals whose composition, due to symmetry constraints, should involve oxygen functions exclusively. (This is strictly valid if *f*-type polarization functions are ignored). All the orbitals of a_1, e, and t_2 symmetry can, in principle, consist of combinations of metal and oxygen functions, but the calculations suggest that only the $3t_2$ and 1e orbitals should be considered strongly M−O bonding.

The $3t_2$ and 1e levels contain substantial contributions from both M d and O p orbitals, whereas in the $2a_1$, $2t_2$, $3a_1$, and $4t_2$ levels, the participation of metal functions is relatively minor and these orbitals appear to be largely of nonbonding (O s or O p) character. The properties of the molecular orbitals of the $[MO_4]^{2-}$ anions therefore suggest a minor participation of metal s and p and oxygen s functions in the bonding interactions.

The metal basis function populations, shown in Table 3, are consistent with the molecular orbital analysis. These results have been obtained by dividing the relative percentage populations

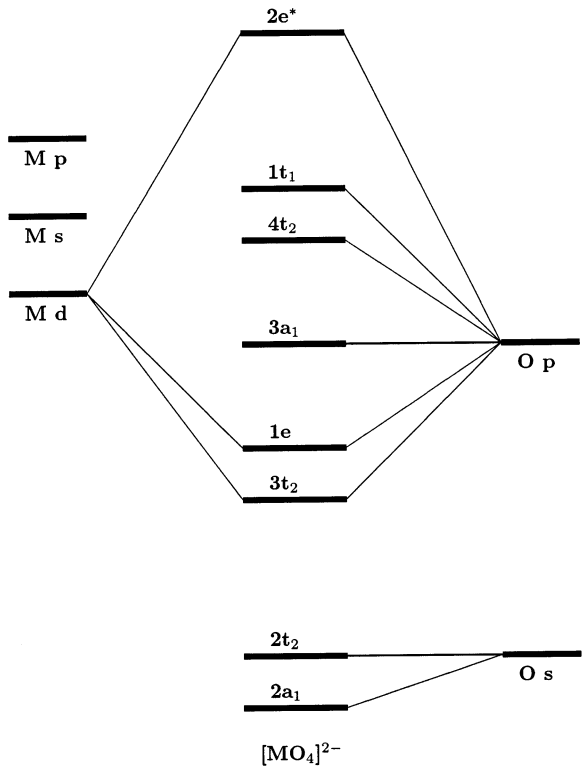

Figure 2. Qualitative molecular orbital diagram showing predominant metal and oxygen contributions to the valence levels of $[MO_4]^{2-}$ anions.

TABLE 4: Mayer M−O Bond Indexes (LDA) for $[MO_4]^{2-}$ Anions

			decomposition			
molecule	basis set	index	a_1	e	t_1	t_2
$[MoO_4]^{2-}$	DZ1P	1.36	0.03	0.48	0.00	0.85
	TZ1P	1.46	0.03	0.48	0.00	0.95
	TZ2P	1.57	0.09	0.48	0.04	0.96
$[WO_4]^{2-}$	DZ1P	1.36	0.08	0.47	0.00	0.81
	TZ1P	1.48	0.08	0.47	0.00	0.93
	TZ2P	1.58	0.11	0.46	0.05	0.96

by the total number of orbitals of a given type. The effects of the basis set on the relative weights of the s, p, and d components are minimal, a dominant d and much smaller s and p contributions being observed in all cases. However, the total population value increases with the number of functions as reflected by the lower charges obtained with larger basis sets.

4.2.1. Bond Indexes and Bonding Energetics. The composition of the molecular orbitals and the population analysis of basis functions can provide useful information about chemical bonding, but a more detailed picture of the relative importance of the different types of orbital interactions can be obtained with bond-order and bonding-energy analyses, particularly through the decomposition of these properties into contributions associated with the irreducible representations of the molecular system.

Mayer indexes for the metal−oxygen interactions in the $[MO_4]^{2-}$ anions are given in Tables 4 and 5. The actual values and relative contributions of the (T_d) symmetry components of the bond orders are also included. Mayer and Muliken analyses are closely connected, and this is observed in the fact that the decrease of the Mulliken charges with basis-set size is reflected by a corresponding increase in the values of the M−O indexes.

The results of the symmetry-based decomposition of the bond orders are in agreement with the conclusions obtained from the molecular-orbital and population analyses. The e and t_2 contributions are considerably higher than the a_1 contribution, as

TABLE 5: Relative (percentage) Contributions of Symmetry Components to Mayer M−O Bond Indexes for $[MO_4]^{2-}$ Anions

molecule	basis set	a_1	e	t_1	t_2
$[MoO_4]^{2-}$	DZ1P	2.2	35.3	0.0	62.5
	TZ1P	2.1	32.9	0.0	65.0
	TZ2P	5.7	30.6	2.6	61.1
$[WO_4]^{2-}$	DZ1P	5.9	34.5	0.0	59.6
	TZ1P	5.4	31.8	0.0	62.8
	TZ2P	7.0	29.1	3.2	60.7

expected from the dominant role of M d-type functions and much more limited participation of M s-type functions in M−O bonding. The more significant values and relative weights of the a_1 indexes obtained with the TZ2P (with respect to the DZ1P or TZ1P) sets correlate with an increase in the population of M s orbitals.

The nonzero t_1 component in the TZ2P indexes is due to the fact that this basis set includes M *f*-type polarization functions which have a small, but not negligible, population (Table 3). The M *f* orbitals transform as the t_1 irreducible representation and, although they are not significantly involved in the M−O chemical bonds (the composition of the $1t_1$ orbitals being approximately 0.99 O and 0.01 M), some minor interaction with O p orbitals occurs and is reflected in the bond-order decomposition.

The calculation of the bonding energetics in a molecular system requires a suitable choice of fragments. An analysis based on equations 10 and 11 involves fragment calculations that must be carried out in a restricted fashion. Therefore, in the case of the $[MO_4]^{2-}$ anions, the most convenient choice for computational purposes is closed-shell species, namely,

$$[M]^{6+} + 4[O]^{2-} = [MO_4]^{2-} \quad \text{(scheme A1)}$$

or

$$[M]^{6+} + [O_4]^{8-} = [MO_4]^{2-} \quad \text{(scheme A2)}$$

These schemes are also convenient from a formal chemical standpoint, particularly for larger systems, as the conservation of (formal) oxidation states is strictly possible.

The orbital-mixing effects in the fragment interactions represented by schemes A1 and A2 can be described as charge transfer from the oxide species to the metal ions. It is also possible to consider electron-pairing effects by using the following decomposition scheme, which has been previously applied to the $[MnO_4]^-$ anion,[5]

$$[M]^{+} + [O_4]^{3-} = [MO_4]^{2-} \quad \text{(scheme A3)}$$

where the electronic configurations of the partially filled shells in the $[M]^+$ and $[O_4]^{3-}$ fragments are respectively $[d^5]$ and $[t_2{}^3e^2]$. These configurations are consistent with the molecular-orbital structure of the bonding in the Mo and W $[MO_4]^{2-}$ anions, which indicates that M−O interactions can be mostly associated with the $3t_2$ and 1e orbitals.

The results obtained from the application of the three different decomposition schemes are summarized in Tables 6 and 7. It should be noted that the analysis based on orbital-mixing energetics includes orbital interactions between fragments and polarization effects represented by the mixing of occupied and unoccupied orbitals in a given fragment due to the presence of the other fragments. Therefore, bonding-energy and bond-order results are not expected to show an exact correspondence, the latter being only associated with the interactions between two

TABLE 6: Energetics (BP86) of Orbital Mixing (ΔE_O in eV) in $[MO_4]^{2-}$ Anions

				decomposition			
molecule	scheme	basis set	ΔE_O	a_1	e	t_1	t_2
$[MoO_4]^{2-}$	*A*1	DZ1P	−64.04	−0.94	−21.25	−1.97	−39.88
		TZ1P	−65.23	−1.03	−21.07	−3.07	−40.06
		TZ2P	−66.09	−1.22	−20.75	−4.03	−40.09
	*A*2	DZ1P	−85.18	−2.87	−25.35	−5.07	−51.88
		TZ1P	−91.23	−2.81	−25.62	−6.61	−56.20
		TZ2P	−92.18	−3.02	−25.30	−7.65	−56.21
	*A*3	DZ1P	−62.54	−0.39	−17.64	−0.68	−43.84
		TZ1P	−62.05	−0.38	−17.23	−0.68	−43.77
		TZ2P	−62.97	−0.48	−17.34	−1.03	−44.11
$[WO_4]^{2-}$	*A*1	DZ1P	−56.89	−1.57	−18.22	−1.94	−35.16
		TZ1P	−58.06	−1.61	−18.03	−3.03	−35.37
		TZ2P	−58.48	−1.64	−17.85	−3.55	−35.44
	*A*2	DZ1P	−77.48	−3.66	−22.05	−4.97	−46.80
		TZ1P	−83.42	−3.71	−22.33	−6.49	−50.89
		TZ2P	−83.94	−3.75	−22.16	−7.06	−50.97
	*A*3	DZ1P	−67.17	−0.67	−18.89	−0.69	−46.92
		TZ1P	−66.48	−0.72	−18.49	−0.69	−46.58
		TZ2P	−66.98	−0.74	−18.58	−0.85	−46.81

TABLE 7: Relative (percentage) Contributions of Symmetry Components to the Orbital Mixing Energies of $[MO_4]^{2-}$ Anions

molecule	scheme	basis set	a_1	e	t_1	t_2
$[MoO_4]^{2-}$	*A*1	DZ1P	1.5	33.2	3.1	62.2
		TZ1P	1.6	32.3	4.7	61.4
		TZ2P	1.8	31.4	6.1	60.7
	*A*2	DZ1P	3.3	29.8	6.0	60.9
		TZ1P	3.1	28.1	7.2	61.6
		TZ2P	3.3	27.4	8.3	61.0
	*A*3	DZ1P	0.6	28.2	1.1	70.1
		TZ1P	0.6	27.8	1.1	70.5
		TZ2P	0.8	27.6	1.6	70.0
$[WO_4]^{2-}$	*A*1	DZ1P	2.8	32.0	3.4	61.8
		TZ1P	2.8	31.1	5.2	60.9
		TZ2P	2.8	30.5	6.1	60.6
	*A*2	DZ1P	4.7	28.5	6.4	60.4
		TZ1P	4.4	26.8	7.8	61.0
		TZ2P	4.5	26.4	8.4	60.7
	*A*3	DZ1P	1.0	28.1	1.0	69.9
		TZ1P	1.1	27.8	1.0	70.1
		TZ2P	1.1	27.7	1.3	69.9

atoms. However, a qualitative or semiquantitative correlation should normally be observed.

The total and partial orbital-mixing (ΔE_O) values vary with the calculation approach employed, due to the different chemical nature of the fragments, but the relative contributions associated with the individual symmetry subspecies are similar in all cases and agree satisfactorily with the molecular-orbital analysis. The orbital-mixing effects are dominated by e and t_2 interactions with minor participation of a_1 and t_1 orbitals.

The basis sets have a rather small effect, in general. The most significant difference between double-ζ and triple-ζ functions is found for scheme A2 and is mostly associated with the t_2 orbitals. This discrepancy appears to be caused by the high charge of the $[O_4]^{8-}$ ion, as the orbital-mixing energy of this fragment has been found to be rather more sensitive to the basis set than those of the $[O]^{2-}$ and $[O_4]^{3-}$ species.

The relative importance of the t_1 contribution is probably the most noticeable difference between bond-order and bonding-energy results. (Even with the DZ1P and TZ1P sets, which do not include metal functions of t_1 symmetry, is a t_1 contribution observed). This is most likely a manifestation of polarization phenomena, which should be involved in the bonding energetics but not in the bond orders.

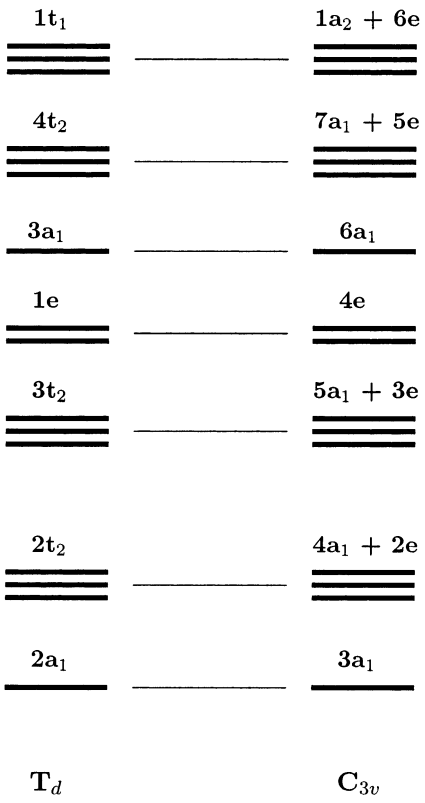

Figure 3. Correlation diagram for the molecular orbital description of $[MO_4]^{2-}$ anions in T_d and C_{3v} symmetry representations.

In general, for all fragment schemes and basis sets, the orbital-mixing results compare well, on a qualitative basis, with the bond-order results. In particular, somewhat closer correlations between the Mayer analysis and bonding energetics of the $[MO_4]^{2-}$ anions are observed for schemes A1 and A2 involving closed-shell species than for scheme A3, which also considers interactions between partially filled shells.

4.2.2. Analysis of Individual Bonds. The t_2 and e orbitals in complexes exhibiting T_d symmetry have sometimes been described as approximately representing σ and π interactions, respectively. However, a definite separation of the σ and π components of individual bonds is not possible if regular tetrahedral symmetry is used.

This can nonetheless be achieved by lowering the symmetry to C_{3v}, as in this case the decomposition of the orbital interactions corresponding to the bond lying along the C_3 axis into their a_1 and e components can be associated with σ and π bonding modes, respectively. This is illustrated by Figures 3 and 4. The a_1 and e orbitals in T_d symmetry conserve their characters in the C_{3v} configuration, whereas the t_2 and t_1 orbitals are split, respectively, into a_1+e and a_2+e contributions.

The calculation of bond indexes only requires that the molecular symmetry be changed from T_d to C_{3v}, but a suitable fragment scheme is needed for the bonding energy analysis. The scheme employed in this work can be represented as

$$[MO_3] + [O]^{2-} = [MO_4]^{2-} \qquad \text{(scheme A4)}$$

where the $[MO_3]$ fragment introduces the required C_{3v} symmetry.

Figure 4 shows that the 1e orbitals (in T_d symmetry) can be considered to represent a π-like bonding mode which is unchanged by the use of the C_{3v} configuration (where they become the 4e orbitals), but that the (T_d) $3t_2$ orbitals which have

TABLE 8: Analysis of σ and π Components (percentage contributions in parentheses) of M−O Bonds in $[MO_4]^{2-}$ Anions[a]

		bonding analysis									
molecule	basis set	β_{MO}	σ	π	η		ΔE_O	σ	π	η	
$[MoO_4]^{2-}$	DZ1P	1.36	0.50	0.86	0.00	(37:63:0)	−11.97	−5.16	−6.78	−0.03	(43:57:0)
	TZ1P	1.46	0.64	0.82	0.00	(44:56:0)	−10.52	−4.74	−5.74	−0.04	(45:55:0)
	TZ2P	1.57	0.71	0.84	0.02	(45:54:1)	−10.71	−4.79	−5.87	−0.05	(45:55:0)
$[WO_4]^{2-}$	DZ1P	1.36	0.49	0.87	0.00	(36:64:0)	−11.81	−5.09	−6.68	−0.04	(43:57:0)
	TZ1P	1.48	0.67	0.81	0.00	(45:55:0)	−10.52	−4.83	−5.64	−0.05	(46:54:0)
	TZ2P	1.58	0.72	0.84	0.02	(46:53:1)	−10.58	−4.83	−5.70	−0.05	(46:54:0)

[a] Bond indexes (β_{MO}) and orbital energies (ΔE_O in eV) correspond to LDA and BP86 calculations, respectively.

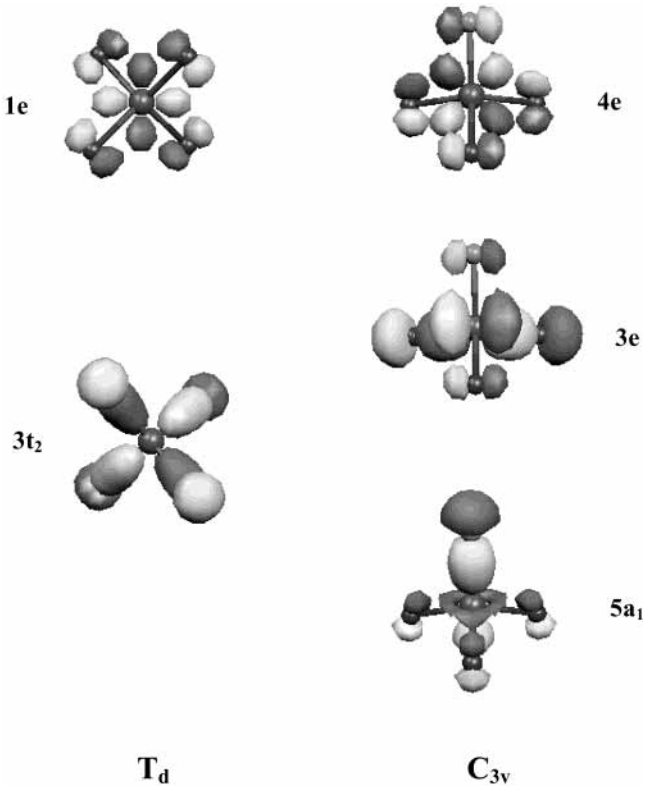

Figure 4. Spatial representation of metal−oxygen bonding orbitals of $[MO_4]^{2-}$ anions.

a predominantly σ-like appearance can be described as a combination of σ bonding, represented by the (C_{3v}) $5a_1$ orbital, and π bonding, represented by the (C_{3v}) 3e orbitals.

An analysis of the σ and π components of the individual M−O bonds in the $[MO_4]^{2-}$ anions is presented in Table 8. This is based on the decomposition of the bond index and orbital-mixing energy into the contributions associated with the irreducible representations in C_{3v} symmetry. The σ-like interactions occur through the mixing of M d_{z^2} and O p_z orbitals which transform as the a_1 species, whereas the π-like bonding modes correspond to M d_{xz}−O p_x and M d_{yz}−O p_y interactions which possess e character. In addition, there are a_2 contributions that are not directly associated with the M−O orbital-mixing effects but can be present as a small component of the bond-order value and the orbital-mixing energy. These a_2 contributions are included in Table 8 as an additional term labeled η.

All the approaches used in the calculation of bond orders and bonding energetics have yielded qualitatively similar results which indicate that the π-like interactions appear to be somewhat more significant than the σ-like interactions. The basis sets utilized in the calculations have an effect on both the bond-order and orbital-mixing values but, with the exception of the DZ1P indexes, the relative (percentage) contributions are only slightly different.

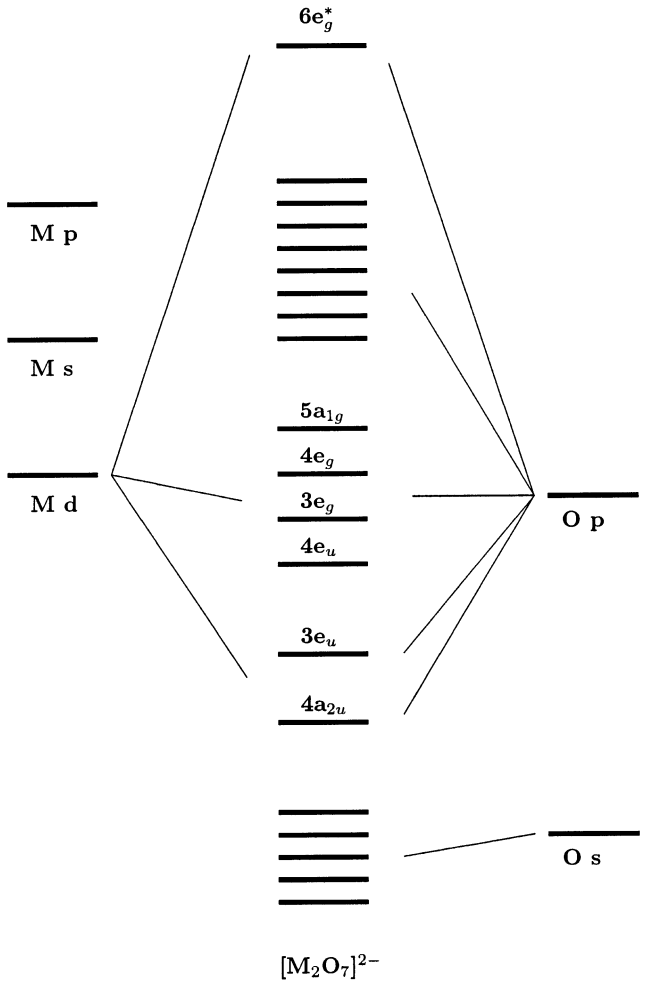

Figure 5. Qualitative molecular orbital diagram showing predominant metal and oxygen contributions to the valence levels of $[M_2O_7]^{2-}$ anions.

The σ component of the Mayer index appears to be most sensitive to the basis functions and, in particular, the value obtained with the DZ1P set is comparatively rather small, and this seems to be the reason the relative contributions calculated with this basis set are significantly different. In the case of the bonding energetics, although the absolute DZ1P values are rather larger than the TZ1P and TZ2P values, the relative σ and π contributions are not strongly affected by the basis set.

4.3. $[M_2O_7]^{2-}$ Anions. A qualitative molecular-orbital diagram showing the metal−oxygen interactions that are most important to chemical bonding in $[M_2O_7]^{2-}$ anions (with D_{3d} molecular symmetry) is given in Figure 5. As observed in the $[MO_4]^{2-}$ species, the orbital structure of bridging and terminal bonds is largely dominated by interactions between M d and O p functions, with a much more limited participation of M s, M p, and O s functions.

TABLE 9: Analysis of σ and π Components (percentage contributions in parentheses) of M−O_b Bonds in $[M_2O_7]^{2-}$ Anions[a]

		bonding analysis									
molecule	basis set	β_{MO}	σ	π	η		ΔE_O	σ	π	η	
$[Mo_2O_7]^{2-}$	DZ1P	0.64	0.29	0.35	0.00	(45:55:0)	−10.84	−5.48	−4.78	−0.58	(51:44:5)
	TZ1P	0.68	0.36	0.32	0.00	(53:47:0)	−9.86	−4.96	−4.27	−0.63	(50:43:7)
	TZ2P	0.77	0.43	0.33	0.01	(56:43:1)	−10.18	−5.05	−4.42	−0.71	(50:43:7)
$[W_2O_7]^{2-}$	DZ1P	0.65	0.30	0.35	0.00	(46:54:0)	−10.83	−5.65	−4.61	−0.57	(52:43:5)
	TZ1P	0.72	0.42	0.30	0.00	(58:42:0)	−10.04	−5.29	−4.12	−0.63	(53:41:6)
	TZ2P	0.83	0.48	0.34	0.01	(58:41:1)	−10.23	−5.32	−4.24	−0.67	(52:41:7)

[a] Bond indexes (β_{MO}) and orbital energies (ΔE_O in eV) correspond to LDA and BP86 calculations, respectively.

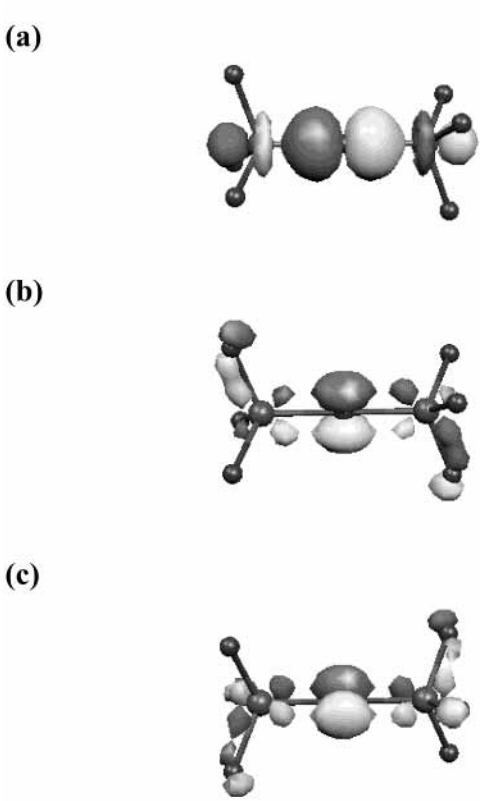

Figure 6. Spatial representation of metal−oxygen bonding interactions in $[M_2O_7]^{2-}$ anions: (a) $4a_{2u}$ orbitals, (b) and (c) $3e_u$ orbitals.

Spatial representations of the three molecular orbitals that are most significant to the description of bridging (M−O_b) bonds are shown in Figure 6. The $4a_{2u}$ orbital corresponds to σ-like interactions involving O_b p_z and M d_{z^2} functions, whereas the $3e_u$ orbitals represent π-like interactions between O_b p_x or p_y functions and M d_{xz} or d_{yz} functions, and also possess some M−O_t bonding character.

An analysis of the σ and π components of the M−O_b bonds can be carried out by considering the contributions to M−O_b bond indexes and orbital-mixing energies associated with the irreducible representations to which the M and O_b basis functions belong. The a_{1g} and a_{2u} symmetry species correspond to M−O_b σ-like interactions (the former being a small contribution in this case as M−O_b σ bonding is predominantly described by the $4a_{2u}$ orbital). The M−O_b interactions of π-like character correspond to the e_u symmetry species.

An analysis of the σ and π components of the M−O_b bonds in the $[M_2O_7]^{2-}$ anions is presented in Table 9. Analogously to the $[MO_4]^{2-}$ species, the bond-order and bonding-energy description of M−O_b interactions may contain small (indirect) contributions, which are most likely linked with polarization functions or polarization effects. In the $[M_2O_7]^{2-}$ molecules, these contributions can be associated with the a_{2g}, a_{1u}, and e_g orbitals and are collectively given in the η term included in Table 9.

The decomposition scheme used for the calculation of the bonding energetics in $[M_2O_7]^{2-}$ anions can be described as

$$2[MO_3] + [O]^{2-} = [M_2O_7]^{2-} \qquad \text{(scheme B)}$$

The general results based on Mayer analysis and bonding energetics largely resemble those obtained for $[MO_4]^{2-}$ anions. All results from calculations employing triple-ζ basis sets suggest that σ-like interactions appear to be somewhat more important than π-like interactions and that the difference between the relative contributions is slightly greater in $[W_2O_7]^{2-}$ than in $[Mo_2O_7]^{2-}$.

The bond-order and orbital-mixing results obtained with the double-ζ basis sets are, however, not consistent with one another. Although the latter are qualitatively equivalent to the predictions based on the calculations carried out with the larger TZ1P and TZ2P sets, the DZ1P Mayer indexes indicate that, along the M−O_b−M bridging unit, π bonding should be more significant than σ bonding. As noted for $[MO_4]^{2-}$ anions, the discrepancies between DZ1P and TZ1P/TZ2P results are probably related to the rather important basis-set dependence shown by the σ component of the M−O bond indexes.

4.4. $[M_6O_{19}]^{2-}$ Polyanions. The polyoxoanions formed by Mo and W are structurally and electronically (much) more complex than the relatively simple four-coordinate species, but the general features of the chemical bonding in the $[MO_4]^{2-}$ and $[M_2O_7]^{2-}$ anions are also observed in the larger $[M_6O_{19}]^{2-}$ clusters. This is illustrated by the qualitative diagram presented in Figure 7, which provides a schematic summary of the predominant character of the orbital interactions in these polyanions.

Chemical bonding in the $[M_6O_{19}]^{2-}$ species can be largely associated with interactions between M d and O p functions, the participation of M s and p orbitals being minor and the O s orbitals being mostly involved in nonbonding combinations that appear as a low-lying "O s band" in the electronic structure.

4.4.1. Orbital Interactions in Terminal Bonds. The levels highlighted in the diagram of Figure 7 represent the only interactions than can be unequivocally ascribed to a particular type of M−O bonds, as the a_{2g}, a_{2u}, and e_u orbitals can only involve bridging atoms due to the O_h symmetry constraints.

An analysis of the σ and π components of the terminal (M−O_t) bonds can nevertheless be performed by using the local C_{4v} symmetry of the $[MO_6]$ polyhedral unit. As in the $[MO_4]^{2-}$ anions, σ-like and π-like interactions can be associated with the a_1 (M d_{z^2}) and e (M d_{xz}, M d_{yz}) contributions to the bond orders and orbital-mixing energies.

The Mayer indexes can be calculated by changing the molecular symmetry from O_h to C_{4v}, and the bonding-energy analysis of M−O_t bonds can be obtained with the fragment scheme represented by

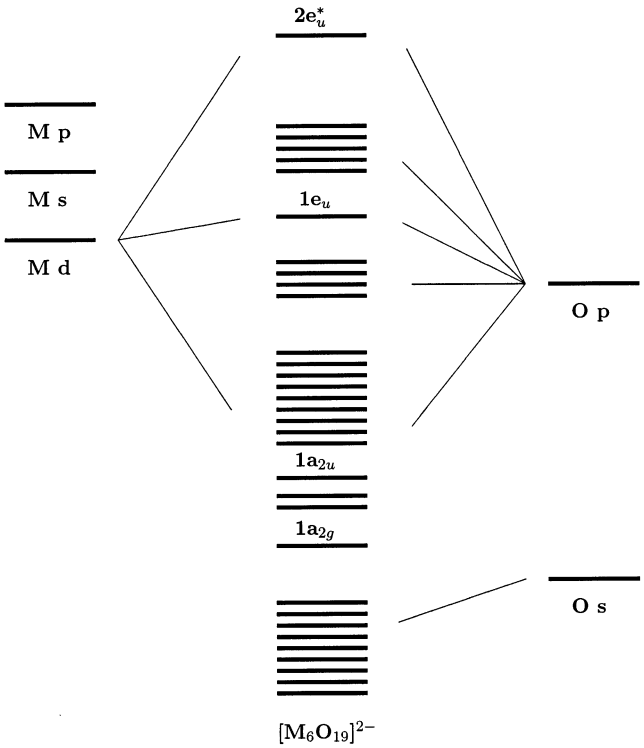

Figure 7. Qualitative molecular orbital diagram showing predominant metal and oxygen contributions to the valence levels of $[M_6O_{19}]^{2-}$ polyanions.

$$[M_6O_{18}] + [O]^{2-} = [M_6O_{19}]^{2-} \quad \text{(scheme C)}$$

where the $[M_6O_{18}]$ fragment introduces the required C_{4v} configuration and the $[O]^{2-}$ ion represents a terminal site.

Table 10 summarizes the bond-order and bonding-energy results obtained for $[M_6O_{19}]^{2-}$ anions. The η term in this case includes the small contributions associated with the a_2, b_1, and b_2 irreducible representations that are not directly related to the major M−O bonding interactions.

All approaches have yielded qualitatively comparable results, suggesting a somewhat more predominant role of π than σ interactions in the terminal bonds. The observed basis-set dependence is similar to those described for the $[MO_4]^{2-}$ and $[M_2O_7]^{2-}$ species, but the differences in the predicted relative contributions of the σ and π components of the bond orders are more significant than those obtained for the smaller anions. However, the cause of these differences can be attributed to the rather strong sensitivity of the σ index to the basis functions used in the calculations, as noted in preceding discussions.

4.4.2. Oxygen Valency and Binding Energy. In addition to calculating orders and interaction energies associated with individual bonds, it is possible to use Mulliken and Mayer data and bonding energetics to explore the general bonding environment of a given atom in a molecule. This can be illustrated by an analysis of the three types of oxygen sites in the $[M_6O_{19}]^{2-}$ polyanions.

As described in the Computational Approach section, the Mayer indexes corresponding to a single atom can be combined to obtain a bond sum or a covalency index, and the integration of Mayer and Mulliken results into a full-valency index can be used as a relative measure of overall bonding capacity. The orbital-mixing energy may display some degree of correlation with the bond sum or the covalency index as it involves "covalent" interactions between fragments, but an exact correspondence is not expected because polarization effects are also included. It may also be possible to observe correlations between full-valency indexes and total bonding energies, as both parameters can be considered to provide a relative measure of the general interactions of an atom or chemical fragment in a molecular environment.

Various oxygen valency indexes calculated using triple-ζ basis sets are given in Table 11. The energetics for the binding of a particular oxygen atom to the polyanion structure can be obtained with scheme C. The results of this fragment analysis are shown in Table 12 and are also used to test the functional dependence of computational bonding energies.

The bond sums and covalency indexes for the various oxygen atoms reflect the nature of the individual M−O interactions. The highest values obtained correspond to the terminal (O_t) sites, which form the strongest covalent bonds and have the lowest Mulliken charges. The bridging (O_b) sites are involved in two relatively strong M−O bonds (of approximately single character) and are also characterized by rather high bond sums and covalency indexes. The internal (O_c) atoms in the $[M_6O_{19}]^{2-}$ polyanions occupy a six-coordinate site and the six individual M−O bonds that they form exhibit noticeably low (∼0.2) orders. However, the high-coordinate environment compensates for the individual bond weakness and the general covalent character of the central atoms is thus significant, albeit smaller than those of the bridging and terminal sites. The full-valency indexes suggest that the overall bonding capacities of the different oxygen types are comparable despite the variety of individual coordination environments and M−O interactions.

The comparison of the TZ1P and TZ2P valency results indicates some dependence on the basis sets used in the calculations. This arises from the separate basis-set effects on Mulliken and Mayer analyses. The individual bond orders obtained with the TZ2P set are higher than those corresponding to the TZ1P set, and so are the resulting bond sums and covalency indexes. The Mulliken charges are influenced by the basis functions used in the calculations, and this should also affect the full-valency values. Nevertheless, the basis-set dependence does not have a considerable effect on the general interpretation of the valency results, as the trends obtained with both TZ1P and TZ2P sets are largely similar.

A correlation between valency analysis and bonding energetics has been observed in previous studies of Nb, Ta, Mo, and W $[M_6O_{19}]^{z-}$ polyanions.[7] This is reproduced by the results shown in Table 12, regardless of the functional employed in the calculations. The orbital-mixing energies correlate with the bond sums and covalency indexes, the highest and lowest values obtained corresponding to terminal and internal oxygen sites, respectively, and the results for bridging atoms being relatively closer to those for the former than the latter. The total bonding energies correlate with the full-valency indexes in that both results suggest that the relative stabilities of the different oxygen sites in the clusters are, to a large extent, comparable even though the general structural and bonding properties of the individual atoms are rather distinct.

The functional effects on the bonding energetics for the oxygen atoms in the $[M_6O_{19}]^{z-}$ anions are minimal, not only on a qualitative basis but also on the quantitative level, as the actual energy values are in all cases largely similar. This observation has been found to be valid for most results obtained using fragment schemes and decomposition analysis of the molecular bonding energy.[31]

4.5. General Remarks. The results obtained for the three types of oxoanions investigated indicate that the agreement between population analysis and bonding energetics is satisfac-

TABLE 10: Analysis of σ and π Components (percentage contributions in parentheses) of M−O_t Bonds in $[M_6O_{19}]^{2-}$ Anions[a]

		bonding analysis									
molecule	basis set	β_{MO}	σ	π	η		ΔE_O	σ	π	η	
$[Mo_6O_{19}]^{2-}$	DZ1P	1.49	0.44	1.05	0.00	(30:70:0)	−19.45	−7.72	−10.74	−0.99	(40:55:5)
	TZ1P	1.68	0.58	1.10	0.00	(35:65:0)	−18.01	−7.40	−9.67	−0.94	(41:54:5)
	TZ2P	1.82	0.72	1.10	0.00	(40:60:0)	−18.24	−7.46	−9.78	−1.00	(41:54:5)
$[W_6O_{19}]^{2-}$	DZ1P	1.50	0.41	1.09	0.00	(27:73:0)	−19.02	−7.70	−10.41	−0.91	(40:55:5)
	TZ1P	1.73	0.63	1.10	0.00	(36:64:0)	−17.67	−7.45	−9.36	−0.86	(42:53:5)
	TZ2P	1.83	0.72	1.11	0.00	(39:61:0)	−17.76	−7.48	−9.39	−0.89	(42:53:5)

[a] Bond indexes (β_{MO}) and orbital energies (ΔE_O in eV) correspond to LDA and BP86 calculations, respectively.

TABLE 11: Valency Indexes for Oxygen Atoms in $[M_6O_{19}]^{2-}$ Anions[a]

molecule	basis set	atom	S_{MO}	C_O	V_O
$[Mo_6O_{19}]^{2-}$	TZ1P	O_t	1.68	2.10	2.30
		O_b	1.50	1.92	2.23
		O_c	1.14	1.41	2.08
	TZ2P	O_t	1.82	2.23	2.37
		O_b	1.60	2.09	2.33
		O_c	1.26	1.58	2.21
$[W_6O_{19}]^{2-}$	TZ1P	O_t	1.73	2.08	2.30
		O_b	1.54	1.88	2.21
		O_c	1.08	1.31	1.99
	TZ2P	O_t	1.83	2.19	2.37
		O_b	1.70	2.11	2.36
		O_c	1.38	1.64	2.19

[a] The bond sum (S_{MO}), covalency (C_O), and full valency (V_O) are calculated from LDA Mayer and Mulliken data.

TABLE 12: Bonding Energetics (eV) of Oxygen Atoms in $[M_6O_{19}]^{2-}$ Anions[a]

molecule	functional	atom	ΔE_O	ΔE_B
$[Mo_6O_{19}]^{2-}$	BP86	O_t	−18.01	−21.62
		O_b	−15.96	−21.21
		O_c	−12.25	−20.20
	BLYP	O_t	−18.05	−21.38
		O_b	−16.03	−20.91
		O_c	−12.24	−19.93
	PW91	O_t	−18.03	−21.79
		O_b	−15.98	−21.42
		O_c	−12.31	−20.43
$[W_6O_{19}]^{2-}$	BP86	O_t	−17.67	−22.50
		O_b	−16.30	−22.17
		O_c	−12.77	−20.77
	BLYP	O_t	−17.72	−22.24
		O_b	−16.36	−21.86
		O_c	−12.75	−20.48
	PW91	O_t	−17.67	−22.67
		O_b	−16.30	−22.38
		O_c	−12.84	−21.00

[a] All results correspond to TZ1P calculations.

tory if basis functions of triple-ζ quality are utilized in the calculations. In general, reasonably good correlations between the two analytical approaches have also been obtained with smaller double-ζ basis sets, but some discrepancies have been found. This can be related to the considerably greater sensitivity of the bond-order and related methods to basis-set quality.

The analysis of the σ and π components of the metal−oxygen bonds provides a suitable example of the quality of the correlations obtained and how these are affected by the choice of basis functions. For calculations employing triple-ζ basis sets, the agreement between bond-order and bonding-energy results is extremely good for $[MO_4]^{2-}$ anions, and is also satisfactory for the $[M_2O_7]^{2-}$ and $[M_6O_{19}]^{2-}$ species. However, for the larger oxoanions, (quantitative) differences of some significance, between the two approaches, are observed.

As noted in preceding discussions, these differences are likely to be connected with the fact that bond-order analysis concentrates on the interactions between two bonded atoms, whereas the calculation of bonding energetics involves, in general, molecular fragments and, thus, in addition to orbital interactions between directly bonded atoms, polarization effects and interactions between nonbonded centers can also be important. These "additional" effects in the bonding energetics can be expected to be more important for larger species, and this is probably the reason the differences between bond-order and bonding-energy results are somewhat greater for $[M_2O_7]^{2-}$ and $[M_6O_{19}]^{2-}$ than for $[MO_4]^{2-}$ systems.

In $[M_2O_7]^{2-}$ and $[M_6O_{19}]^{2-}$ anions, the (η) term that measures indirect bonding effects is a small but significant component of the orbital-mixing energy, whereas its contribution to the bond-order values is negligible. This difference in the magnitude of the η term affects the calculation of the relative contributions associated with σ and π interactions and leads to the observed discrepancies between the bond-order and bonding-energy analyses. In $[MO_4]^{2-}$ anions, the incidence of the η term in the results from both approaches is extremely small and, thus, the calculated relative contributions of the σ and π bonding modes are largely similar.

In calculations that utilize double-ζ basis sets, there is an additional factor that affects the correlations between bond-order and bonding-energy analyses. These smaller basis sets have yielded orbital-mixing results similar to those obtained with the triple-ζ sets, but have consistently given lower values for the σ component of the bond index. This has led to less satisfactory agreement between the two approaches and, in the case of the $[M_2O_7]^{2-}$ anions, to a qualitative discrepancy in the prediction of the relative importance of the σ and π components of the M−O_b−M bonds.

5. Conclusion

It has been mentioned in the Introduction that the combination of population analyses of molecular orbitals with bonding energy decomposition approaches has been described as an excellent method for the study of chemical bonding interactions in molecular systems. An extended population analysis, which includes bond and valency indexes, can (significantly) enhance the description of the chemical bonding in molecular species, as it provides details about the nature of the interactions between bonded atoms and an indication of the bonding capacity of individual atoms.

The preferred approach to the computational analysis of chemical bonding should be a combination of the various population, molecular-orbital, and bonding-energy methods. For the three groups of Mo and W oxoanions studied, all of these methods have provided qualitatively consistent descriptions of the bonding interactions and properties, for calculations employing basis sets of moderate size (which corresponds to triple-ζ quality). The use of smaller basis sets has led to some discrepancies, whereas the functional influence has been, in general, minimal.

It is important to note that although a combined approach should provide the most detailed description, this can be difficult to achieve for some particular species. The calculation of bond orders and related properties can be advantageous in that it is computationally more economical and can be more widely applied than the methods based on bonding energetics. Bond indexes can be obtained for species of any molecular symmetry and can be highly useful as a means of quantifying bonding interactions in systems of low symmetry, for which the fragment calculations required to obtain information on bonding energetics can be difficult or not possible.

Acknowledgment. The authors thank EPSRC and the University of Hull for financial support, and the Computational Chemistry Working Party for access to computational facilities in the Rutherford Appleton Laboratory.

References and Notes

(1) Koch, W.; Holthausen, M. C. *A Chemist's Guide to Density Functional Theory*, 2nd ed.; Wiley VCH: Weinheim, 2001.

(2) Parr, R. G.; Yang, W. *Density-Functional Theory of Atoms and Molecules*; Oxford University Press: New York, 1989.

(3) Stowasser, R.; Hoffmann, R. *J. Am. Chem. Soc.* **1999**, *121*, 3414.

(4) Kar, T.; Angyan, J. G.; Sannigrahi, A. B. *J. Phys. Chem. A* **2000**, *104*, 9953.

(5) Bickelhaupt, F. M.; Baerends, E. J. *Rev. Comp. Chem.* **2000**, *15*, 1.

(6) Bridgeman, A. J.; Cavigliasso, G. *Polyhedron* **2001**, *20*, 3101.

(7) Bridgeman, A. J.; Cavigliasso, G. *Inorg. Chem.* **2002**, *41*, 1761.

(8) Bridgeman, A. J.; Cavigliasso, G. *J. Chem. Soc., Dalton Trans.* **2002**, 2244.

(9) Bridgeman, A. J.; Cavigliasso, G. *Inorg. Chem.* **2002**, *41*, 3500.

(10) Bridgeman, A. J.; Cavigliasso, G. *J. Phys. Chem. A* **2002**, *106*, 6114.

(11) Bridgeman, A. J.; Cavigliasso, G. *Polyhedron* **2002**, *21*, 2201.

(12) Mayer, I. *Chem. Phys. Lett.* **1983**, *97*, 270.

(13) Evarestov, R. A.; Veryazov, V. A. *Theor. Chim. Acta* **1991**, *81*, 95.

(14) Landrum, G. A.; Goldberg, N.; Hoffmann, R. *J. Chem. Soc., Dalton Trans.* **1997**, 3605.

(15) Baerends, E. J.; Ellis, D. E.; Ros, P. *Chem. Phys.* **1973**, *2*, 41.

(16) Versluis, L.; Ziegler, T. *J. Chem. Phys.* **1988**, *88*, 322.

(17) teVelde, G.; Baerends, E. J. *J. Comput. Phys.* **1992**, *99*, 84.

(18) FonsecaGuerra, C.; Snijders, J. G.; teVelde, G.; Baerends, E. J. *Theor. Chem. Acc.* **1998**, *99*, 391.

(19) teVelde, G.; Bickelhaupt, F. M.; Baerends, E. J.; FonsecaGuerra, C.; van Gisbergen, S. J. A.; Snijders, J. G.; Ziegler, T. *J. Comput. Chem.* **2001**, *22*, 931.

(20) Bridgeman, A. J.; Empson, C. J. MAYER; University of Hull: Kingston upon Hull, UK, 2002.

(21) MOLEKEL: An Interactive Molecular Graphics Tool; Portmann S.; Lüthi, H. P. *CHIMIA* **2000**, *54*, 766.

(22) Vosko, S. H.; Wilk, L.; Nusair, M. *Can. J. Phys.* **1980**, *58*, 1200.

(23) Kohn, W.; Sham, L. J. *Phys. Rev.* **1965**, *140*, A1133.

(24) Becke, A. D. *Phys. Rev. A* **1988**, *38*, 3098.

(25) Perdew, J. P. *Phys. Rev. B* **1986**, *33*, 8822.

(26) Lee, C.; Yang, W.; Parr, R. G. *Phys. Rev. B* **1988**, *37*, 785.

(27) Perdew, J. P.; Wang, Y. *Phys. Rev. B* **1992**, *45*, 13244.

(28) Bridgeman, A. J.; Cavigliasso, G. *Polyhedron* **2001**, *20*, 2269.

(29) Bridgeman, A. J.; Cavigliasso, G. *J. Phys. Chem. A* **2001**, *105*, 7111.

(30) Bridgeman, A. J.; Cavigliasso, G., Ireland, L. R.; Rothery, J. *J. Chem. Soc., Dalton Trans.* **2001**, 2095.

(31) Cavigliasso, G. PhD Thesis, University of Cambridge, 2002.